Generalized Photoelectromagnetic Effect in Semiconductors

D. L. Lile
Naval Electronics Laboratory Center, San Diego, California 92152
(Received 20 April 1973)

The photoelectromagnetic (PEM) response of high-purity single-crystal n-type InSb has been measured over the temperature range 80–300 °K. A comparison of the data with the results of a theoretical treatment of the PEM effect, generalized to include bulk generation at arbitrary magnetic field, gives values for the surface-recombination velocity on this material both as a function of temperature and of surface preparation. The results also include the first reported observation of a negative PEM response due to the diffusion of carriers into recombination sites at the illuminated sample surface.

I. INTRODUCTION

The photoelectromagnetic (PEM) effect [sometimes called the photomagnetoelectric (PME) effect] has long enjoyed popularity as a technique for the measurement of bulk- and surface-recombination rates in semiconductors. The effect was first observed by Kikoin and Noskov[1] in Cu_2O and explained in terms of a photodiffusion of excess electron-hole pairs by Frenkel[2] in 1934. Little interest was shown in the effect, however, until Aigrain and Bulliard[3] reported PEM data on single-crystal samples of Ge in 1953 and Moss *et al.*[4] published a somewhat more rigorous theoretical treatment of the phenomenon in the same year. Measurements of the PEM effect have since been reported on PbS,[5,6] Si,[7] intrinsic and p-type InSb,[8] InAs,[9] CdS,[10] and semiconducting and semi-insulating single crystals of GaAs.[11–13] For the interested reader a review of this early work appears in the article by Garreta and Grosvalet.[14] Advances in a theoretical understanding have been no less extensive. Notable among these are the treatments of Kurnick and Zitter[15] and van Roosbroeck[16] which have enjoyed outstanding success in explaining much of the observed PEM data reported to date. The effects of large levels of carrier injection, where trapping[17] and nonlinear recombination may become important, have been treated by Beattie and Cunningham,[18] Agraz and Li,[19] and Li and Huang.[20]

Common to all of these analyses, however, is the assumption that photon absorption and thus carrier generation, occurs at the illuminated surface of the semiconductor. For all the data presently available this assumption would seem to be adequate. Gärtner[21] has presented a theory for the PEM effect in the presence of volume generation but has restricted the treatment to the case of small magnetic fields.

This paper presents the results of an experimental and theoretical study of the PEM effect in n-type InSb over the temperature range from 80 to 300 °K. The first section of the paper will present a theory for the PEM effect in the presence of bulk-carrier generation, finite sample thickness and arbitrary magnetic field. It will be shown (and later demonstrated) that under certain experimental conditions, which can for example be readily achieved in InSb, the PEM signal may be expected to reverse polarity. Following a summary of the relevant bulk parameters of InSb and a discussion of the experimental techniques employed in this study the final section of the paper will present the results of PEM measurements made on bulk high-purity n-type samples of InSb as a function of magnetic induction and temperature. From these results, values of the surface recombination velocity will be determined as a function of temperature and for various techniques of surface preparation.

II. THEORY

The present treatment of the PEM effect is based on the following assumptions: (i) Steady-state conditions prevail; (ii) the injected carrier density is small compared to the thermal equilibrium concentration; (iii) the thermal equilibrium carrier concentration is independent of position, i.e., the effects of built-in electric fields are neglected; (iv) nondegenerate carrier statistics apply; (v) the sample is sufficiently large that edge effects are negligible and thus that a one-dimensional analysis may be applied; (vi) all materials parameters are independent of magnetic field.

With reference to Fig. 1 the current components in the semiconductor may be written

$$J_{hx} = qp\mu_h E_x + \mu_h B J_{hy}, \tag{1}$$

$$J_{hy} = qp\mu_h E_y - \mu_h B J_{hx} - qD_h \frac{\partial p}{\partial y}, \tag{2}$$

$$J_{ex} = qn\mu_e E_x - \mu_e B J_{ey}, \tag{3}$$

$$J_{ey} = nq\mu_e E_y + \mu_e B J_{ex} + qD_e \frac{\partial n}{\partial y}, \tag{4}$$

where J_e and J_h are the electron and hole current densities, respectively; the x and y components being indicated by subscripts. n and p are the electron

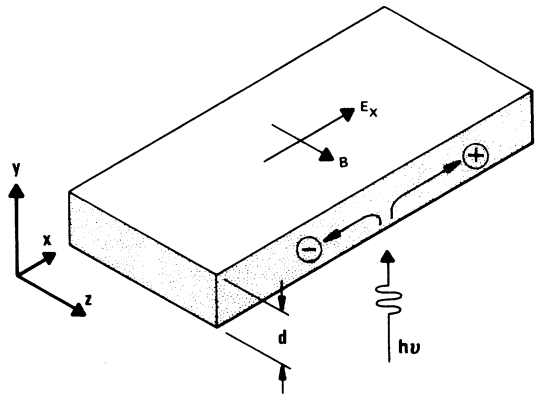

FIG. 1. Schematic representation of sample configuration and electron-hole pair separation leading to the generation of the normal PEM effect. The coordinate axes and magnetic field orientation used in the present theoretical treatment are as shown. Illumination is incident in the y direction onto the semiconductor surface lying in the xz plane at $y=0$, the resulting PEM field E_x being generated along the x axis.

and hole concentrations, μ_e and μ_h the carrier mobilities, D_e and D_h are the diffusion coefficients, q is the magnitude of the electronic charge, B is the magnetic field (in the z direction), and E_x and E_y are the x and y components of the electric field. Eliminating J_{hx} between Eqs. (1) and (2) and J_{ey} between Eqs. (3) and (4) and eliminating E_y between the two resulting equations gives the equation for the current density in the y direction,

$$J[p\mu_h(1+\mu_e^2B^2)+n\mu_e(1+\mu_h^2B^2)] = qnp\mu_e\mu_h(\mu_e+\mu_h)BE_x + q\left(n\mu_eD_h\frac{\partial p}{\partial y}+p\mu_hD_e\frac{\partial n}{\partial y}\right). \quad (5)$$

In Eq. (5), $J=J_{ey}=-J_{hy}$ as a result of the fact that the current density $(J_{ey}+J_{hy})$ must vanish at the surface and hence, under steady-state conditions, in the interior also.

Assuming that the carrier generation rate due to optical excitation decreases exponentially with distance into the sample, the current continuity equation may be written

$$\frac{\partial J}{\partial y}=\frac{q}{\tau_{PEM}}\left(\frac{np-n_0p_0}{n_0+p_0}\right)-qAe^{-\alpha y}, \quad (6)$$

where n_0 and p_0 are the thermal equilibrium electron and hole concentrations, α is the absorption coefficient, A is the electron-hole pair generation rate per unit volume at the illuminated surface, and τ_{PEM} is the effective recombination time for injected carriers in a PEM measurement and is given in terms of the lifetimes of electrons and holes τ_n and τ_p by[17]

$$\tau_{PEM}=\frac{n_0\tau_p+p_0\tau_n}{n_0+p_0}. \quad (7)$$

Taking the derivative of Eq. (6) gives

$$\frac{\partial^2 J}{\partial y^2}=\frac{q}{\tau_{PEM}}\left(\frac{n\partial p/\partial y+p\partial n/\partial y}{n_0+p_0}\right)+q\alpha Ae^{-\alpha y}. \quad (8)$$

With the assumption of carrier nondegeneracy (which has been universally assumed in all previous treatments if not always explicitly stated) the diffusion coefficients appearing in Eq. (5) may be related to mobility through the Einstein relation. This allows Eqs. (5), (6), and (8) to be combined to give

$$L_D^2\frac{\partial^2 J}{\partial y^2}+\tau_{PEM}\mu_e(\mu_e+\mu_h)BE_x\frac{\partial J}{\partial y} - \left(\frac{p\mu_h(1+\mu_e^2B^2)+n\mu_e(1+\mu_h^2B^2)}{\mu_h(n_0+p_0)}\right)J = -\frac{qn_0p_0\mu_e(\mu_e+\mu_h)BE_x}{(n_0+p_0)}+A\tau_{PEM}\mu_e \times e^{-\alpha y}[\alpha kT-q(\mu_e+\mu_h)BE_x], \quad (9)$$

where L_D is the electron diffusion length and k is Boltzmann's constant. For $\alpha\to\infty$, i.e., surface generation, Eq. (9) reduces directly to Eq. (6) of Ref. 15.

Following Kurnick and Zitter[15] Eq. (9) may be linearized by assuming small-signal conditions so that n and p may be replaced by their thermal equilibrium values in the coefficient of J. Furthermore if

$$\tau_{PEM}\mu_e(\mu_e+\mu_h)BE_x \ll L_D\left(\frac{p_0\mu_h(1+\mu_e^2B^2)+n_0\mu_e(1+\mu_h^2B^2)}{\mu_h(n_0+p_0)}\right)^{1/2}, \quad (10)$$

then the term in $\partial J/\partial y$ may be neglected. The inequality (10) is well satisfied in all cases to be considered in this paper.

With these provisions, Eq. (9) reduces to a standard linear differential equation of second order whose solution is

$$J=C_1e^{ay}+C_2e^{-ay}+\frac{qn_0p_0\mu_e(\mu_e+\mu_h)BE_x}{a^2L_D^2(n_0+p_0)} - \frac{A\tau_{PEM}\mu_e[\alpha kT-q(\mu_e+\mu_h)BE_x]e^{-\alpha y}}{L_D^2(a^2-\alpha^2)}, \quad (11)$$

where

$$a=\left(\frac{p_0\mu_h(1+\mu_e^2B^2)+n_0\mu_e(1+\mu_h^2B^2)}{L_D^2\mu_h(n_0+p_0)}\right)^{1/2}.$$

a^{-1} (which has been termed[17] the effective ambipolar magnetic diffusion length) reduces, at low B, to the normal ambipolar diffusion length.

C_1 and C_2 appearing in Eq. (11) are constants of integration which must be determined from the

boundary values imposed on the solution. Conventionally the boundary condition at a surface is specified in terms of an effective surface-recombination velocity S through an equation of the form

$$J_{\text{surf}} = qS\left(\frac{np - n_0 p_0}{n_0 + p_0}\right)_{\text{surf}} . \tag{12}$$

In addition the current continuity equation (6) must still be satisfied, thus the boundary conditions are

$$J\Big|_{y=0} = S_1 \tau_{\text{PEM}}\left(\frac{\partial J}{\partial y}\Big|_{y=0} + qA\right)$$

and (13)

$$J\Big|_{y=d} = -S_2 \tau_{\text{PEM}}\left(\frac{\partial J}{\partial y}\Big|_{y=d} + qA\, e^{-\alpha d}\right) ,$$

where S_1 and S_2 are the values of S at $y = 0$ and d, respectively. These boundary conditions suffice to determine C_1 and C_2 uniquely.

Working towards a solution for the PEM voltage, two cases are of interest. When the PEM signal generated along the x axis of the sample is measured with a meter whose impedance is much less than that of the sample, E_x is reduced to zero (the so-called short-circuit case) and from Eqs. (1) and (3) the measured current per unit sample width is given by

$$J_{\text{SC}} = \int_0^d (J_{ex} + J_{hx})\, dy = -B(\mu_e + \mu_h) \int_0^d J\, dy . \tag{14}$$

For low-impedance bulk samples it is usually far simpler experimentally to determine the PEM signal with a measuring device whose impedance is much larger than that of the sample. In this case

$$\int_0^d (J_{ex} + J_{hx})\, dy = 0,$$

and from Eqs. (1) and (3) the PEM open-circuit field E_x is given by

$$E_{\text{OC}} = \frac{B(\mu_e + \mu_h)}{q(n_0 \mu_e + p_0 \mu_h) d} \int_0^d J\, dy . \tag{15}$$

Following considerable (although quite routine) algebraic manipulation it follows from Eqs. (11) and (13)–(15) that

$$J_{\text{SC}} = \frac{-qAB(\mu_e + \mu_h)\mathfrak{R}}{a(a^2 - \alpha^2)\left[a\tau_{\text{PEM}}(S_1 + S_2)\cosh(ad) + (1 + S_1 S_2 a^2 \tau_{\text{PEM}}^2)\sinh(ad)\right]} , \tag{16}$$

where

$$\mathfrak{R} = \left[(\alpha - S_2 a^2 \tau_{\text{PEM}}) + (\alpha + S_1 a^2 \tau_{\text{PEM}}) e^{-\alpha d}\right]\cosh(ad)$$
$$- a\left[(1 - S_2 \alpha \tau_{\text{PEM}}) - (1 + S_1 \alpha \tau_{\text{PEM}}) e^{-\alpha d}\right]\sinh(ad) - \left[(\alpha + S_1 a^2 \tau_{\text{PEM}}) + (\alpha - S_2 a^2 \tau_{\text{PEM}}) e^{-\alpha d}\right] \tag{16a}$$

and

$$E_{\text{OC}} = \frac{AB(\mu_e + \mu_h)\mathfrak{R}}{(a^2 - \alpha^2)(n_0 \mu_e + p_0 \mu_h) d\xi} , \tag{17}$$

where

$$\xi = a[a\tau_{\text{PEM}}(S_1 + S_2)\cosh(ad) + (1 + S_1 S_2 a^2 \tau_{\text{PEM}}^2)\sinh(ad)] - \frac{\mu_e(\mu_e + \mu_h)^2 B^2}{a^2(a^2 - \alpha^2) L_D^2 d (n_0 + p_0)(n_0 \mu_e + p_0 \mu_h)}$$
$$\times \Big\{(a^2 - \alpha^2) n_0 p_0 \{2 - [2 - a^2 d \tau_{\text{PEM}}(S_1 + S_2)]\cosh(ad) - a[\tau_{\text{PEM}}(S_1 + S_2) - d(1 + S_1 S_2 a^2 \tau_{\text{PEM}}^2)]\sinh(ad)\}$$
$$- A\tau_{\text{PEM}} a^2 (n_0 + p_0)\left[\left(\frac{a}{\alpha}(1 - e^{-\alpha d})[S_1 S_2 \tau_{\text{PEM}}^2(\alpha^2 - a^2) - 1] + a\tau_{\text{PEM}}(S_2 + S_1 e^{-\alpha d})\right)\sinh(ad)\right.$$
$$\left. + \left(\frac{(S_1 + S_2) a^2 \tau_{\text{PEM}}}{\alpha}(e^{-\alpha d} - 1) + \alpha\tau_{\text{PEM}}(S_1 - S_2 e^{-\alpha d}) + (e^{-\alpha d} + 1)\right)\cosh(ad) - [(1 + S_1 \alpha\tau_{\text{PEM}}) + e^{-\alpha d}(1 - S_2 \alpha\tau_{\text{PEM}})]\right]\Big\} . \tag{17a}$$

Equations (16) and (17) describe, respectively, the short-circuit current and open-circuit PEM field generated in a slab of material of arbitrary thickness d. They are valid for all values of magnetic field and absorption coefficient consistent with our implicit neglect of quantum phenomena and reflections at the rear surface of the sample. For small magnetic fields and low photon flux densities (i.e., B and $I \to 0$) they reduce directly to the expressions [Eqs. (21) and (22) of Ref. 21] derived by Gärtner. From the complexity of ξ alone it is evident that these equations cannot easily be handled in an analytic fashion. In the limit of $\alpha \to \infty$ and $ad \gg 1$, i.e., surface absorption and a sample thick with respect to a diffusion length

$$\mathfrak{R} \to \tfrac{1}{2} e^{ad} \alpha(1 + S_2 a \tau_{\text{PEM}}) \tag{18}$$

and

$$J_{SC} \to \frac{q\eta(1-R)IB(\mu_e+\mu_h)}{a(1+S_1 a\tau_{PEM})} , \tag{19}$$

where $I=A[\alpha\eta(1-R)]^{-1}$ is the photon flux density incident on the sample, η is the quantum efficiency, and R is the reflectivity of the semiconductor. Equation (19) is identical to that derived by Kurnick and Zitter [Eq. (7) of Ref. 15].

Furthermore,

$$\xi \to \frac{a}{2} e^{ad}(1+S_1 a\tau_{PEM})(1+S_2 a\tau_{PEM})\left[1-\frac{\mu_e(\mu_e+\mu_h)^2B^2}{aL_D^2(n_0\mu_e+p_0\mu_h)}\left(\frac{n_0p_0}{a(n_0+p_0)}+\frac{I\tau_{PEM}(1+S_1\alpha\tau_{PEM})}{\alpha d(1+S_1 a\tau_{PEM})}\right)\right] \tag{20}$$

and

$$E_{OC}=-\eta(1-R)IB(\mu_e+\mu_h)\left\{ad(n_0\mu_e+p_0\mu_h)(1+S_1 a\tau_{PEM})\left[1-\frac{\mu_e(\mu_e+\mu_h)^2B^2}{aL_D^2(n_0\mu_e+p_0\mu_h)}\left(\frac{n_0p_0}{a(n_0+p_0)}+\frac{I\tau_{PEM}(1+S_1\alpha\tau_{PEM})}{\alpha d(1+S_1 a\tau_{PEM})}\right)\right]\right\}^{-1}. \tag{21}$$

If I is sufficiently small that the last term in Eq. (20) may be neglected then from Eqs. (19) and (21)

$$\left.\frac{J_{SC}}{E_{OC}}\right|_{\alpha\to\infty,\, ad\gg 1} = qd(n_0\mu_e+p_0\mu_h) \times\left(1-\frac{n_0p_0\mu_e(\mu_e+\mu_h)^2B^2}{a^2L_D^2(n_0+p_0)(n_0\mu_e+p_0\mu_h)}\right), \tag{22}$$

which is simply the conductance of unit width of the sample in a magnetic field B. This was observed previously by Kurnick and Zitter.[15]

With the above assumption that carrier generation occurs at the surface (i.e., $\alpha\to\infty$) carrier flow at all points within the sample must be away from the illuminated surface. As can be seen from Eq. (21) (as well as from a qualitative consideration of Fig. 1) the polarity of the resulting PEM field is negative with the presently assumed coordinate axes. This will be referred to as the *normal* PEM effect and is what has been experimentally reported in all previous discussions of the PEM effect. If instead α is finite so that bulk generation occurs, then any recombination at the front surface will result in some carrier flow towards the illuminated surface. If this component of current flow exceeds that away from the front surface due to diffusion and recombination at the back surface, then the net current flow will be towards the illuminated surface and the PEM voltage will be of the opposite polarity. With the present sign convention E_{OC} will be positive. This will be referred to as the *negative* PEM effect. Gärtner[21] has suggested that for the observation of such an effect the excess carrier density at the illuminated surface must be less than that at the rear surface. A necessary but insufficient condition for this is that $S_1>S_2$. It is further necessary that ad be not too much larger than unity. If this latter condition is not satisfied then carriers will be able to recombine via bulk centers before reaching the unilluminated surface of the sample. In this way the excess carrier density at the rear surface of the sample will approach zero irrespective of the value of S_2. This will necessarily preclude the generation of a smaller carrier excess at the illuminated surface.

Inspection of Eq. (17a) indicates that at low temperatures, where n_0p_0 is small, the quadratic term in B in ξ may in general be neglected compared with the first term for all readily accessible values of magnetic field. Furthermore if I is small, specifically if

$$I \ll \frac{n_0p_0\,\alpha d(1+S_1 a\tau_{PEM})}{a\tau_{PEM}(n_0+p_0)(1+S_1\alpha\tau_{PEM})} ,$$

then

$$\xi \to a[a\tau_{PEM}(S_1+S_2)\cosh(ad)+(1+S_1S_2a^2\tau_{PEM}^2)\sinh(ad)].$$

ξ is thus positive for all values of S_1 and S_2 and hence the sign of E_{OC} is determined by $\mathcal{R}$.

If $\alpha\gg a$ and $\alpha d\gg 1$, then from Eq. (16a)

$$\mathcal{R} \to (\alpha - S_2a^2\tau_{PEM})\cosh(ad)+S_2a\alpha\tau_{PEM}\sinh(ad)-(\alpha+S_1a^2\tau_{PEM}) \tag{23}$$

and

$$E_{OC} \to \frac{-\eta IB(\mu_e+\mu_h)[(\alpha-S_2a^2\tau_{PEM})\cosh(ad)+S_2a\alpha\tau_{PEM}\sinh(ad)-(\alpha+S_1a^2\tau_{PEM})]}{\alpha ad(n_0\mu_e+p_0\mu_h)[a\tau_{PEM}(S_1+S_2)\cosh(ad)+(1+S_1S_2a^2\tau_{PEM}^2)\sinh(ad)]} \tag{24}$$

If $S_1\gg(a\tau_{PEM})^{-1}$ and $S_2\ll(a\tau_{PEM})^{-1}$, then

$$E_{OC} \to \frac{-\eta IB(\mu_e+\mu_h)\{\alpha[\cosh(ad)-1]-S_1a^2\tau_{PEM}\}}{\alpha a^2d(n_0\mu_e+p_0\mu_h)S_1\tau_{PEM}\cosh(ad)} . \tag{25}$$

From this equation it can be seen that the open-circuit PEM voltage goes to zero for

$$S_1=\alpha[\cosh(ad)-1]/a^2\tau_{PEM} . \tag{26}$$

For values of S_1 less than this the net carrier

flow is away from the illuminated surface and the normal PEM effect prevails. However, for S_1 larger than the value given by Eq. (26) the net carrier flow will be towards the front surface of the sample and the negative PEM effect with a reversed sign of the generated voltage will occur. If S_2 is finite, then the value of S_1 required for the observation of the negative PEM effect will be larger than that given by Eq. (26). One should note however, from Eq. (26), that whereas S_1 may be sufficiently large to generate a negative PEM effect at wavelengths near the fundamental edge where α is small, it may be of insufficient magnitude to maintain the effect at shorter wavelengths. This problem of the spectral dispersion of the PEM effect has been discussed at some length by Gärtner[21] and has been recently studied in Ge via a measurement of the magnetic flux generated by the circulating PEM current.[22]

Using the parameter values for InSb given in Sec. III, Eq. (26) suggests that in a sample 340 μm thick the recombination velocity on the front surface must be greater than $\sim 3.5\times10^5$ m/sec at 90 °K for the observation of the negative PEM effect at low values of magnetic field. If $S_1 \to \infty$ then the negative PEM field will approach asymptotically a value

$$E_{OC}(S_1 \to \infty) = \frac{\eta I B(\mu_e + \mu_h)}{\alpha d(n_0\mu_e + p_0\mu_h)\cosh(ad)} . \quad (27)$$

Normalizing this maximum negative PEM field to the maximum normal PEM field available with $S_1 = 0$, as given by Eq. (24) with $S_1 = S_2 = 0$, gives

$$\left.\frac{E_{OC}(S_1 \to \infty)}{E_{OC}(S_1 = 0)}\right|_{S_2=0} = -\frac{a\sinh(ad)}{\alpha\cosh(ad)[\cosh(ad)-1]} . \quad (28)$$

If $\mu_h B \ll 1$ (for $n_0 \gg p_0$ and $\mu_e \gtrsim \mu_h$), then a is practically independent of magnetic field, and from Eq. (24) it can be seen that E_{OC} is essentially linear in B. However as B increases and a begins to increase with B, the value of S_1 required for the observation of the negative PEM effect will rapidly increase [Eq. (26)]. Thus a sample with a sufficiently large value of S_1 for the observation of the negative PEM effect at low magnetic field may revert to the normal PEM effect as B is increased.

Of considerable practical interest is the case where d is small. This, of course, has specific relevance to the application of the present theory to the case of thin films of semiconductors. If the assumption made previously, namely that $\alpha d \gg 1$, still applies, and further if $ad \ll 1$, then equality (26) reduces to

$$S_1 = \alpha d^2/2\tau_{PEM} . \quad (29)$$

If $S_2 > 0$, then from Eq. (24) E_{OC} goes to zero for

$$S_1 = \alpha d(S_2 + d/2\tau_{PEM}) . \quad (30)$$

For a 5-μm-thick film of InSb at 90 °K this suggests that the negative PEM effect will be observed with $S_2 = 0$ at short wavelengths for all $S_1 \gtrsim 20$ m/sec. Recombination at the rear surface of the film will however, markedly increase this low threshold value.

As an illustration of the above, Fig. 2 shows E_{OC} versus S_1 calculated using Eq. (17) with $S_2 = 0$. The material parameters used are those appropriate to n-type InSb at 88 °K. A doping density of 10^{14} cm^{-3} was assumed and α was taken as 1.4×10^6 m^{-1}, a value appropriate to illumination at a wavelength of ~ 1.7 μm. It is evident from this figure, as well as Eqs. (26) and (28), that the negative PEM effect will manifest itself both at a lower value of S_1 as well as with a larger magnitude as sample thickness d is reduced.

Although the above treatment has concentrated on the behavior of the open-circuit PEM effect similar

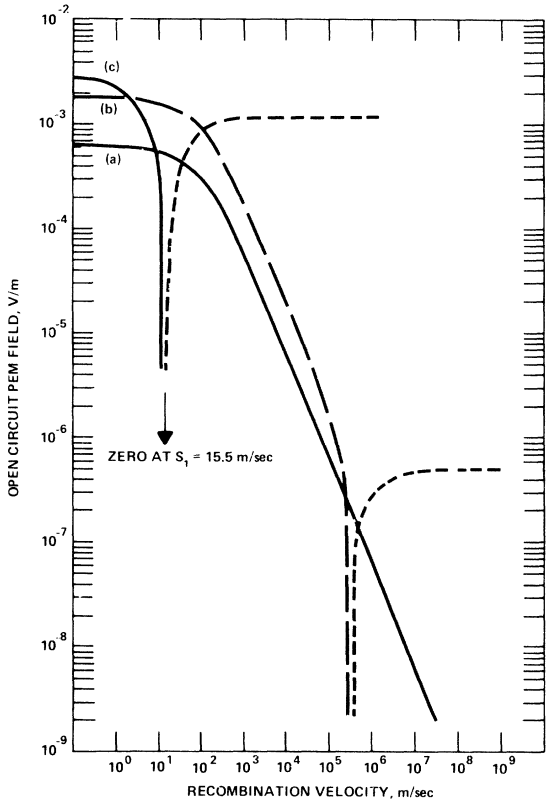

FIG. 2. Theoretical variation of the open-circuit PEM field with surface-recombination velocity for InSb samples of thickness 1 mm [curve (a)], 340.0 μm [curve (b)], and 5.0 μm [curve (c)]. The curves were calculated using Eq. (17) with bulk parameter values appropriate to InSb at 88 °K. An illumination intensity of 1 W/m^2 at 1.65 μm and a magnetic field of 0.1 Wb/m^2 was assumed. The recombination rate on the rear surface was taken as zero. Signals corresponding to the negative PEM effect are shown by the short dashed lines.

results may be obtained from a consideration of the short circuit case given by Eq. (16).

III. BULK PARAMETERS OF InSb

Any attempt at a precise study of the electrical properties of a surface requires, *a priori*, accurate data on the bulk parameters of the sample under investigation. In preparation for the PEM results to be presented in Sec. V it will prove convenient to summarize here what is felt to be the best currently available data on the bulk properties of single-crystal n-type InSb of relevance to the present investigation. The reader interested in a more general review of the properties of InSb is referred to the comprehensive studies by Hilsum and Rose-Innes[23] and Madelung.[24]

A. Electron Carrier Concentration and Mobility

These parameters were measured directly on the samples used in this study. A Van der Pauw Hall measurement was made as a function of temperature on the slice of semiconductor from which the samples were subsequently cut. The results of this measurement for $B \sim 2$ kG are shown in Fig. 3. It can be seen that the Hall coefficient varies as is to be expected and indicates for this sample a net donor density of $\sim 1.05 \times 10^{14}$ cm^{-3}. Furthermore, the electron mobility values shown in Fig. 3(b) are in very good agreement with currently available data on pure material[23,24] and follow closely the form $\mu_e = 1.09 \times 10^9 T^{-1.68}$ cm^2/V sec suggested by Hrostowski *et al.*[25] for lattice dominated scattering in InSb.

The values of μ_e shown are based on a value of the Hall coefficient factor $r(B)$ of unity.[26] The results of Hilsum and Barrie[27] show that the Hall coefficient in pure n-type material ($n < 10^{14}$ cm^{-3}) at room temperature is essentially independent of magnetic field suggesting that $r = 1.0$. At 77 °K Beer[28] has reported a value for r which decreases from a value of 1.1 for $B \lesssim 50$ G to unity for $B \gtrsim 2$ kG. Similar results as well as an unexplained increase in R_H for fields in excess of ~2 kG have been reported by Bate *et al.*[29] These results are in agreement with the theoretical analysis of Ehrenreich[30] which shows that for intrinsic material, where screened polar optical mode scattering combined with electron-hole scattering dominates, $r(0)$ increases from a value of ~1.01 at 300 °K to ~1.07 at 200 °K. These results thus suggest that, at least over the temperature range 80–300 °K, $r(B)$ has a value near to unity for $B \gtrsim 2$ kG.

B. Hole Carrier Concentration and Mobility

For temperatures in excess of ~170 °K the present samples are intrinsic and $p_0 = n_0$. To determine the hole concentration at lower temperatures in the extrinsic range requires a knowledge of the intrinsic carrier density n_i from which $p_0 = n_i^2/n_0$ may then be calculated (within the limitations of carrier nondegeneracy). No experimental data exists on n_i at low temperatures; however, given a knowledge of the carrier effective masses m_e

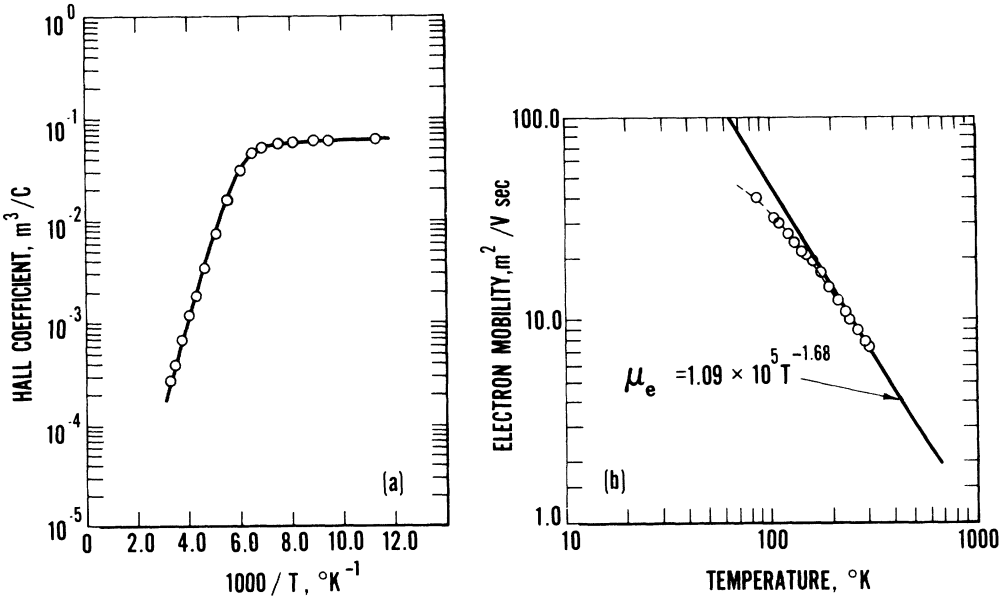

FIG. 3. Temperature dependence of the Hall coefficient (a) and electron mobility (b) as measured on the single-crystal slice of n-type InSb from which the PEM samples were cut. The data shown were obtained from a Van der Pauw measurement made in a magnetic field of 0.185 Wb/m^2.

and m_h and thermal energy gap $E_g(T)$, it may be calculated using

$$n_i^2 = 4(2\pi kT/h^2)^3 (m_e m_h)^{3/2} e^{-E_g(T)/kT}. \quad (31)$$

To within an accuracy of better than 10%[31] the electron effective mass may be assumed temperature independent with a value of $0.013m_0$. In the absence of any experimental data to the contrary m_h is also assumed temperature independent with a value of $0.4m_0$. Using these values of the effective masses together with the band-gap data of Roberts and Quarrington[32] n_i was calculated using Eq. (31). Although this approach will only give an approximate value for p_0 it suffices for the present purposes owing to the relative insensitivity of the PEM signal to the minority carrier concentration at low temperatures.

The hole mobility in n-type material is perhaps the least well known bulk parameter of InSb. The results of Hrostowski *et al.*[25] on p-type material indicate that lattice scattering dominates for $T \gtrsim 100$ °K for the purest specimen studied ($p \sim 3\times10^{14}$ cm^{-3}). Both their data as well as that of Howarth *et al.*[33] may be fitted by an expression of the form

$$\mu_h = 1.25\times10^8 T^{-2.097} \text{ cm}^2/\text{V sec} \quad (32)$$

at high temperature. The impurity density in the present material is less than that reported for their p-type samples and furthermore the impurities are donors. Because of this, as well as the lack of a preferable alternative, the assumption will be made that lattice dominated scattering will exist for holes to the lowest temperatures studied and that in consequence, Eq. (32) may be taken to describe μ_h over the entire experimental range.

C. Carrier Lifetime

Considerable data exists in the literature on the carrier recombination time in both p- and n-type InSb. Furthermore a good qualitative and quantitative agreement exists between much of this data regarding the mechanisms and magnitude of carrier recombination and trapping which occurs in this material. At temperatures below ~ 200 °K recombination is believed to occur via one or more trapping levels, although as yet no consensus would seem to exist on the exact nature of these centers. Above 200 °K the lifetime is believed to be limited by direct interband Auger recombination. A result of this is that at low temperatures trapping plays a dominant role in the recombination process in p-type material and $\tau_p \gg \tau_n$ (typically[34] $\tau_p \sim 4\times10^{-6}$ sec and $\tau_n \sim 5\times10^{-10}$ sec at 77 °K). In n-type material and in p-type above ~ 200 °K trapping can be neglected so that τ_n equals τ_p and, from Eq. (7), also equals τ_{PEM}. A composite of the available experimental data suggests a recombination time in n-type InSb which varies with temperature as shown in Fig. 4. This plot is based on all available data of which the author is aware. However, five papers[34–38] were of special significance because their authors reported lifetime values over a wide temperature range. All remaining references[39] give spot values at either 300 or 77 °K. Of these, those on p-type material using the PEM-Photoconductivity ratio method[15] to measure lifetime at low temperature were discounted because of trapping.[17] The vast majority of the remaining data was within ±20% of the values shown in Fig. 4. The data shown are felt to be particularly representative of material of net donor doping $\lesssim 5\times10^{14}$ cm^{-3}. Also shown in Fig. 4 is the theoretical Auger lifetime as calculated by Beattie and Landsberg.[40] One can see that the fit with experiment is extremely good at the higher temperatures.

D. Optical Parameters

Sample reflectivity and absorption coefficient affect directly both the number and the distribution of injected electron-hole pairs in the specimen. Values of these parameters for InSb have been reported by a number of authors both as a function of wavelength and of sample purity. Much of this data however, is limited to wavelengths near the fundamental edge where α is relatively small or

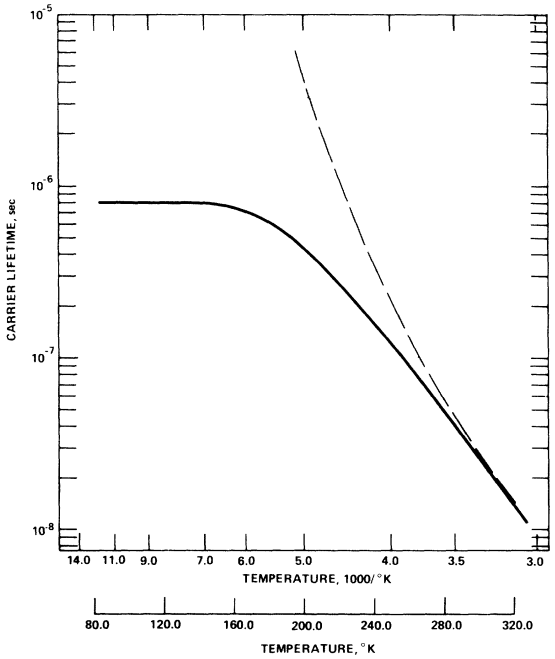

FIG. 4. Temperature dependence of carrier lifetime in n-type InSb. Solid curve is a composite based on the available data in the literature (see text) and the dashed curve is the theoretical Auger lifetime calculated by Beattie and Landsberg (Ref. 40).

is made on impure material where the Burstein-Moss shift exerts a considerable effect. Seraphin and Bennett,[41] in a review article, have summarized and tabulated the available optical constants n and k of a number of semiconductors. Their data for InSb at short wavelength is taken from the work of Philipp and Ehrenreich[42] which gives $\alpha = 1.36\times10^4$ cm^{-1} and $R = 36.8\%$ for InSb at 1.65 μm, the wavelength at which the majority of the present measurements were made. Moss *et al.*[43] report $\alpha = 1.5\times10^4$ cm^{-1}, and the results of Gobeli and Fan[44] give $\alpha \sim 2\times10^4$ cm^{-1} (by extrapolation) at 1.65 μm. At this wavelength the data of Kesamanly *et al.*[45] give $\alpha \sim 1.0\times10^4$ cm^{-1} and $R \sim 36\%$. By a somewhat extravagant extrapolation (from 5 μm) the present authors obtain a value of $R \gtrsim 37\%$ from the data of Spitzer and Fan.[46] All of these results were reported on intrinsic n-type material at room temperature. In the light of the above results a value of $\alpha = 1.4\times10^4$ cm^{-1} and $R = 37\%$ will be taken as representative for InSb at 1.65 μm. Furthermore although both these parameters will vary with temperature, the dependence is expected to be slight and will be neglected. Some support for this is obtained from the results of Gobeli and Fan[44] where α at short wavelength varied by $\lesssim 10\%$ on going from room to liquid-nitrogen temperature. Any variations in the optical properties between samples resulting from different techniques of surface preparation will also be neglected.[41]

In addition to n and k (or R and α) it is necessary [Eqs. (19) and (21)] to know the quantum efficiency for photon to electron conversion. Very little data exists in the literature on this parameter for InSb. In the absence of an extensive concensus the data of Tauc and Abraham[47] will be taken as definitive, which gives at room temperature and 0.75 eV an internal quantum efficiency of 125%. Any dependence of this parameter on temperature will also be neglected.

IV. EXPERIMENTAL PROCEDURE

Samples of InSb were prepared from commercially available single-crystal material of net donor doping $\sim 1.0\times10^{14}$ cm^{-3} (Fig. 3). Material of this purity is nondegenerate for all temperatures $\lesssim 280$ °K. Rectangular specimens approximately $0.4\times1.0\times10$ mm were cut with a wire saw so that the large surfaces were oriented parallel to the (331) crystal plane. These surfaces were then ground flat using a 600-mesh (15-μm particle size) alumina slurry on a glass plate. Following this one surface was prepared in one of the following ways.

(i) The surface was polished with a No. 2 alumina abrasive (0.3-μm particle size) in water. This technique gave a highly reflective surface which nevertheless contained a large number of fine scratches.

(ii) Following polishing as in (i) the surface of the sample was wiped for approximately 30 sec with a cotton swab soaked in a 1–5% solution of bromine in methanol. The treatment was terminated by flooding the sample surface with liberal quantities of methanol. This procedure minimizes the exposure of the surface to air while it is in contact with the bromine and thus reduces the formation of any surface oxide. In this way a surface of good optical quality was obtained essentially free from scratches. Microscopic examination, however, revealed a large number of narrow elongated indentations or rilles in the surface. Not unreasonably it would seem that the swabbing resulted in either an uneven application of pressure over the surface or in a nonuniform exposure of the surface to the etchant.

(iii) Following polishing as in (i) the sample was immersed and agitated for approximately 30 sec in a 1–5% bromine in methanol solution in a plastic beaker. The etch was terminated by flushing the solution with Methanol as in (ii).

(iv) After preparing the surface as described in either (ii) or (iii) above, the sample was anodized to 20 V in a 0.1N aqueous solution of KOH. Following all of the above the samples were given a final rinse in flowing deionized water ($\rho \gtrsim 18.0$ MΩ cm).

Soldered indium contacts were applied to both ends of each sample. These contacts were determined to be ohmic at all temperatures from the linear and symmetric nature of the current voltage characteristics of the samples as well as from the consistent agreement of the measured resistance with that calculated from the measured Hall mobility and carrier concentration. During the optical measurements the contacts were masked with black tape to eliminate their making any contribution to the measured photosignals. The samples were mounted in an evacuated stainless-steel Dewar which fitted between the pole pieces of an 8 kG electromagnet. The magnet was driven by a stabilized power supply which held magnetic field variations to < 1%. The magnet was calibrated using a Hall probe gaussmeter. The copper mount holding the samples, and presumably the samples themselves, was temperature controlled by a proportional controller which maintained temperature constant to within ±0.5 °K over the range from ~ 80 to ~ 310 °K. Illumination for the measurements was obtained from either a microscope lamp or a Nernst glower. The light was mechanically chopped at ~ 500 Hz and then passed through a prism monochromator. The output from the monochromator, which for most of the measurements were set at 0.75 eV (1.65 μm), was collected and focused onto the sample by a large aperture front

silvered mirror. Illumination of the sample was made at normal incidence through either a NaCl or soda glass window in the Dewar. For some of the measurements a Corning glass filter was fitted over the Dewar window to eliminate stray light. The photon flux in the beam from the monochromator was determined by replacing the Dewar with a thermocouple detector which had been calibrated against a standard black-body source. The transmittance of the Dewar windows and the filter was also measured using the thermocouple and was allowed for in calculating the light intensity reaching the samples. The system was aligned each time a sample was replaced by adjusting the focussing mirror to give a maximum PEM signal. The sample was assumed to be at the prime focus when this condition was satisfied. Although considerable effort was taken with the optical system, it is felt that the dominant experimental inaccuracy results from an inability to precisely determine the illumination intensity on the sample. This problem will be discussed more fully in Sec. V.

The photosignals generated by the samples were measured using a PAR model 124 phase-locked amplifier. Because the resistance of the samples was low (typically $\lesssim 50\Omega$ at 80 °K) the open-circuit PEM voltage rather than the short circuit current was measured using a PAR model-116 preamplifier with an input impedance of 100 MΩ.

V. EXPERIMENTAL RESULTS AND DISCUSSION

The results of this investigation fall logically into two distinct categories. The first involves those samples whose surfaces were prepared by one of the first three techniques discussed in Sec. IV. The second group contains those results obtained on surfaces which have been anodized.

A. PEM Results on Free-Surface Samples

Figure 5 shows the results of the open circuit PEM measurements made on a number of samples of InSb over the temperature range 80–300 °K. The data were obtained at a magnetic field of 1.36 kG and an illumination intensity of a few 100 μW/cm^2.

To facilitate easy comparison between samples and with theory all data have been normalized to an illumination intensity of 1.0 W/m^2. Also shown in the figure is a set of theoretical curves calculated using Eq. (17) for various values of surface recombination velocity S_1 on the illuminated surface. Bulk parameter values used were those presented in Sec. III. It is to be noted that the difference between using the full expression for the PEM field [Eq. (17)] and the usually employed approximation [Eq. (21)] is completely negligible in this region, namely, where the surface-recombination velocity is not too large and the sample thickness, which is typically 340 μm in the present case, is much larger than the absorption length of the light and not small compared to a diffusion length. Furthermore, the effect of changes in S_2 in this region can also be neglected. The calculated PEM signal was found to only increase by a couple of percent if S_2 was changed from zero to 10^6 m/sec. The curves shown in Fig. 5 were calculated with $S_2 = 0$.

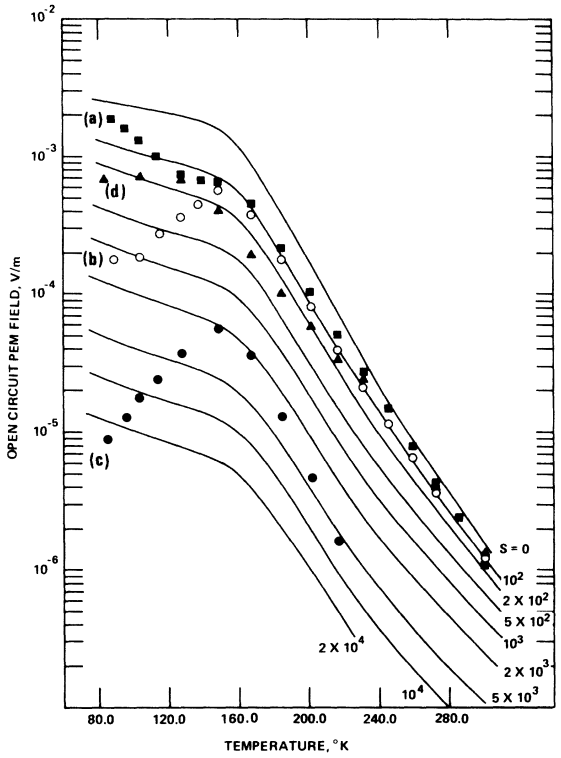

FIG. 5. Temperature dependence of the open circuit PEM field for an illumination intensity of 1 W/m^2 at 1.65 μm and a magnetic field of 0.136 Wb/m^2. Solid curves are theory using Eq. (17) with various values of S_1 (in m/sec) as shown and S_2 equal to zero. Sample thickness was taken as 340.0 μm and all remaining parameters were assigned values as discussed in the main text. The data points correspond to samples prepared as follows: The solid block points [curve (a)] are for a sample swilled in a bromine in methanol solution. Open circles [curve (b)] are for a sample whose surface was prepared by swabbing with bromine in methanol and the solid circles [curve (c)] were obtained on a sample polished with a No. 2 alumina abrasive. The solid triangular points [curve (d)] were measured on a sample whose surface was first polished in bromine in methanol and subsequently subjected to a plasma discharge in dried N_2.

It can be seen that the results for sample B102* [curve (a)] approach very closely the theoretical

curve for zero surface-recombination velocity, whereas curve (b) for sample B102 departs significantly from the zero S curve for temperatures less than ~150 °K. Curve (c) for sample B102+, prepared by mechanical polishing [surface technique (i)] can be seen to depart appreciably from the zero S_1 curve over the entire temperature range studied. It should be appreciated that although a number of samples were used, in a few cases one sample was prepared with one surface finish and measured. Following this it would be removed from the Dewar and reprocessed with a different surface technique. This is the case for curves (a)–(c) in Fig. 5 which were all measured on the same sample but after different surface treatments. Curve (b) is for a bromine in methanol swabbed surface [technique (ii)] and curve (a) is for a subsequent swill in bromine in methanol [technique (iii)]. *It should be mentioned that the good agreement between theory and experiment obvious in Fig. 5 for the most highly polished samples attests not only to the adequacy of the theoretical model but also to the mutual consistency of the presently available bulk data on this material.*

A comparison of the theoretical and experimental curves in Fig. 5 allows the surface-recombination velocity for each sample to be determined as a function of temperature. The results of this are shown in Fig. 6. It is felt to perhaps be of some significance that all these curves show an inflexion point near the temperature range over which the samples change from intrinsic to extrinsic. Although the agreement between the results on the bromine in methanol treated surface and the theoretical curve for zero recombination velocity are excellent, the accuracy of the measurement only allows for limited interpretation. As was stated in Sec. IV, it is felt that the greatest error is involved in the determination of the photon flux incident on the samples. It is estimated that from one sample to the next, as well as during the course of one measurement, the relative illumination intensity can be determined to better than ± 5%, however, the absolute magnitude of the photon flux can only be determined to within perhaps ±15%. This presents no real problem for samples whose surface-recombination rate is large; from Eqs. (19) and (21) it can be seen that for $S_1 \gg (a\tau_{PEM})^{-1}$ the PEM voltage varies inversely with S_1 and a 15% error in the former results in the same error in the deduced recombination velocity. However, if $S_1 < (a\tau_{PEM})^{-1}$ the dependence of the PEM signal on S_1 is reduced. It can be seen in Fig. 5 that for $S_1 \lesssim 2\times 10^2$ m/sec the theoretical curves are closely spaced. At room temperature a 15% error in E_{oc} results in a resolution limit or uncertainty on S_1 of ~60.0 m/sec. At lower temperatures where τ_{PEM} is larger, this same error results in a resolution of $\lesssim$ 20.0 m/sec. This resolution limit for the present experiment is shown by the dashed line in Fig. 6. It was also taken into account in drawing the curves (a) and (b) in this figure which are averages and do not reflect the scatter in the deduced S values below 10^2 m/sec. It should be appreciated that although there is a relatively large uncertainty in the magnitude of S_1 as determined by this technique when $S_1 < (a\tau_{PEM})^{-1}$ the variation of S_1 with temperature can be accepted with

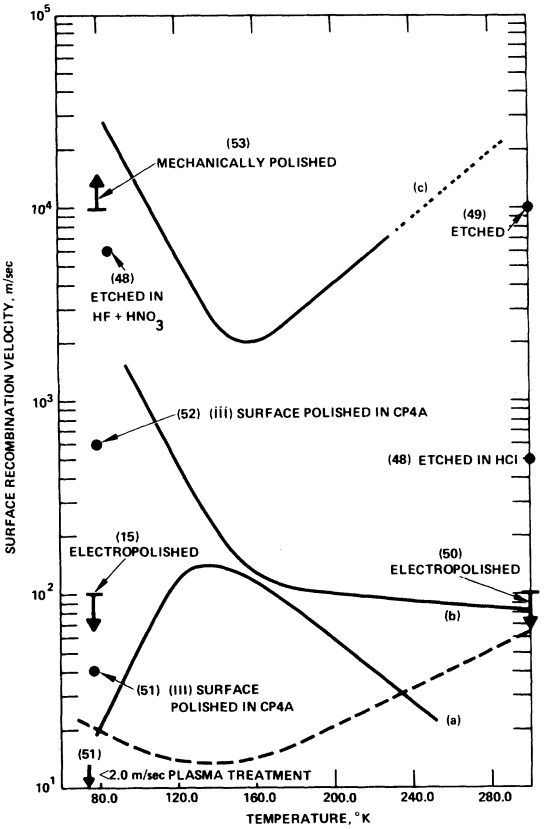

FIG. 6. Variation of the surface-recombination velocity of n-type InSb with temperature as determined from the PEM data in Fig. 5. Curve (a) is for a surface prepared by swilling in bromine in methanol. Curve (b) is for a sample prepared by swabbing the surface with bromine in methanol, and curve (c) is for a surface polished with 0.3-μm particle size alumina. The dashed line shows the resolution limit on S set by an estimated 15% experimental error in measuring the PEM signal and the short dashed line represents a linear extrapolation to room temperature of the data on the mechanically polished sample. Previously published values of S are shown by the full circles together with a reference number and the preparative technique employed. Although unreported in the original paper, the samples of Ref. 53 were prepared by mechanical polishing. If the reported value of S was given only as a maximum or minimum value this is indicated by an arrow.

some confidence. It is conservatively estimated that during one temperature run (which takes ~2 h) the experimental conditions change by less than 5% and in consequence it is felt that the peak in S shown by curve (a) in Fig. 6 can be accepted as real. In addition to the present data, Fig. 6 also includes all previously published values of S for InSb of which this author is aware.[15,48-53] Although the spread is wide, it is to be noted that all previously reported values lie within the limits set by the present results for a polished surface [curve (c)] and a chemically etched surface [curve (a)]. Of this previously available data, that of Davis[51] is most interesting. Davis reported a marked reduction in surface-recombination velocity following plasma treatment of an InSb sample in a dried-N_2 environment. This technique was tried in the present study using a spark-plug-generated discharge in the Dewar in which the samples were mounted. Although no extensive investigation of this technique was made owing to its limited practicability, in no case could the recombination rate be reduced below the best achievable with the bromine in methanol etching technique. Worse, however, was the fact that if the discharge was initiated after the sample was cooled to ~80 °K the results became very unstable changing markedly and irreproducibly with time at the lowest temperatures. This problem seemed not to occur if the discharge was generated prior to cooling the sample. The results obtained in this case are shown by curve (d) in Fig. 5. Although the present attempt using this technique does not fully support the results reported by Davis, it is felt that this may result from differences in experimental procedure. Davis did not report extensively on the technique and in the present case, no effort was taken to clean the Dewar to prevent sputtering of impurities onto the sample from the walls of the enclosure. If performed in a quartz Dewar, for example, this process might produce results equal to or better than those achieved by a bromine in methanol etch.

It should be added that although a very low value of S could be achieved by polishing in the present case, the results at low temperature where the samples are extrinsic did change slightly with subsequent cycles of heating and cooling. The general tendency observed was that S increased slightly for $T \lesssim 160$ °K each time the sample was warmed to room temperature and then recooled. Above a temperature of 160 °K no changes were observed and after two or three temperature cycles the low-temperature behavior also became stable with a value of S lying somewhere between that obtained on a freshly prepared surface [curve (a) in Figs. 5 and 6] and a "swabbed" surface [curve (b)]. Changes similar to this have been observed previously in n-type material at low temperature.[36,51]

B. PEM Results on Anodized Samples

The surface potential of InSb when in contact with its anodic oxide may be readily changed by exposing the semiconductor to radiation of energy greater than ~1.5 eV. By combining radiative exposure with a subsequent thermal treatment, the surface may be "cycled" from flat band through inversion and back to flat band (for n-type material and *vice versa* for p-type) in much the same way as the gaseous cycle studied by Brattain and Bardeen[54] applied to Ge. This phenomenon, which has been explained in terms of an optically activated transfer of electrons from the surface of the InSb into traps in the anodic oxide, has been studied by a number of workers. Most recently Lile[55] has presented data on the photovoltage generated at the anodized surface of InSb from which were deduced values of surface-recombination velocity as large as 5×10^6 m/sec at 80 °K. These results were, however, based on a number of rather debatable assumptions as well as an involved theory. The present study was initially undertaken in an attempt to verify this previous data on S using the hopefully far less ambiguous PEM response.

Figure 7 shows the open circuit PEM field generated in a sample of InSb which had, following polishing in bromine in methanol, been anodized to 20 V in a 0.1N aqueous solution of KOH (producing ~600 Å of oxide[55]). The window of the Dewar was initially covered with a filter which excluded light of energy $\gtrsim 1.0$ eV. The sample was then cooled and the PEM response measured. At ~80 °K the window was removed and the room lights were turned on. Sufficient radiation of energy >1.5 eV could then reach the sample to cause the PEM signal to go through zero to a value of the opposite sign as shown in Fig. 7. This was allowed to continue (typically ~10 min) until no further change was observed. The room lights were then turned off and the filter replaced. The PEM response was then measured as the sample was warmed to room temperature.

Because neither the reflectance nor absorptance of the anodic oxide is known it was not possible to determine the intensity of illumination reaching the InSb. It was felt, however, that at the higher temperatures the response of the anodized surface should not be markedly different to that of the free polished surface and so the data shown in Fig. 7 represent the result of a fit of curve (b) to the theoretical curve (a) for $S_1 = 0$. The data following low-temperature exposure of the sample to room light were adjusted by the same amount. The fit, which corresponds to an additional loss of ~46% of the light over that which would be reflected at a free InSb surface, is felt to be justified by the

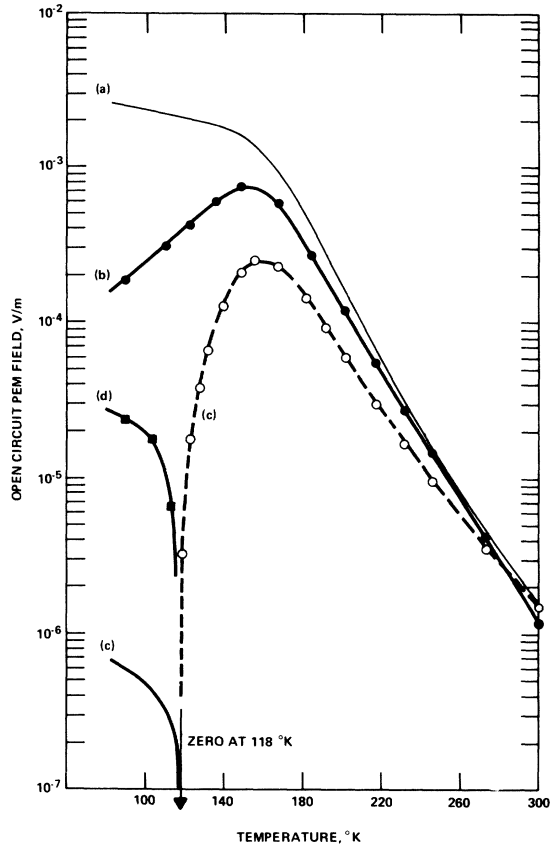

FIG. 7. Variation of the open circuit PEM field with temperature for an anodized sample of InSb. Curve (a) is the theoretical variation calculated using Eq. (17) with $S_1 = S_2 = 0$. The full circles are data points measured on the unexposed sample and the open circles and block points are those measured following exposure of the surface to room light. The full curve (b) and the full and dashed curves (c) are theoretical, calculated using Eq. (17) with the values of S_1 shown in Fig. 8. Both the block data points [curve (d)] and the theoretical curve (c) below 118 °K correspond to the negative PEM effect. Data, taken in a magnetic field of 0.136 Wb/m^2, have been normalized to an illumination intensity of 1 W/m^2 at 1.65 μm.

resulting good agreement of experiment with theory over the studied temperature range above 180 °K.

By comparing these results with theory, it is possible to determine S_1 for the anodized surface both before and after exposure to room light. This was done graphically in the same manner as for the unanodized samples (Fig. 5), and the results are shown in Fig. 8. It can be seen that whereas the results before exposure are essentially identical (subject to the validity of the fitting involved) with those on the unanodized surface (Fig. 6), after exposure the effective recombination rate rises dramatically with decreasing temperature. The lines (b) and (c) in Fig. 7 represent a plot of Eq. (17) with the values of S_1 given in Fig. 8. It is to be noted that whereas an excellent fit can be achieved with the data for the normal sign of the PEM response it is not possible to precisely fit the negative PEM data. The experimentally measured negative PEM response following room light exposure at 80 °K exceeds the theoretical limit given by Eq. (27). Although this cannot be accounted for at this time it may be due to the inadequacy of the theory in not including the effects of the drift term in the diffusion equation [assumption (iii)]. In the presence of large surface-space-charge fields, as are present in the anodized InSb system following exposure to room light, [55] this assumption may no longer be valid. [56,57]

In the light of this limitation it was felt to be unrealistic to postulate values for S in this negative PEM region. However, from Eq. (26) and as is shown in Fig. 8, it would seem that S_1 at low temperature exceeds a value of $\sim 5\times10^5$ m/sec as is required for the observation of a negative PEM

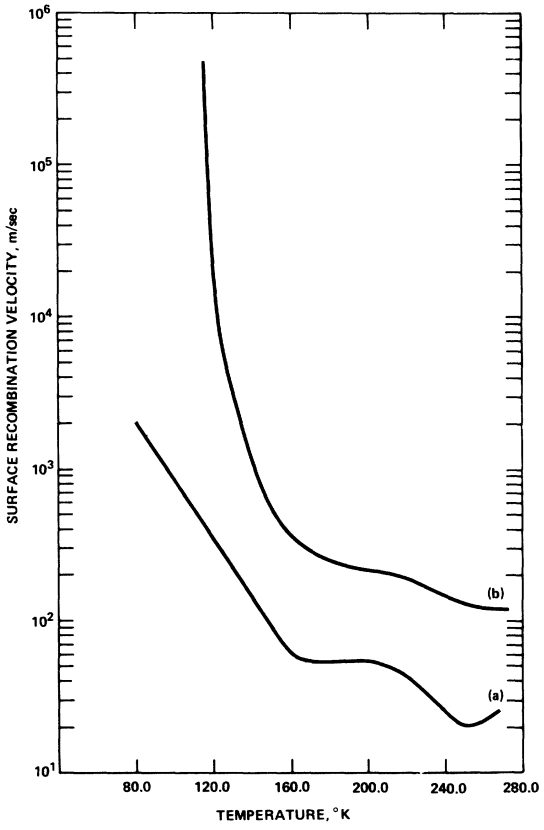

FIG. 8. Surface-recombination velocity at the anodized InSb surface deduced from a comparison of the experimental data shown in Fig. 7 with the theoretically expected open-circuit PEM field given by Eq. (17). Curve (a) is for the unexposed sample and curve (b) is for the surface following exposure to room light.

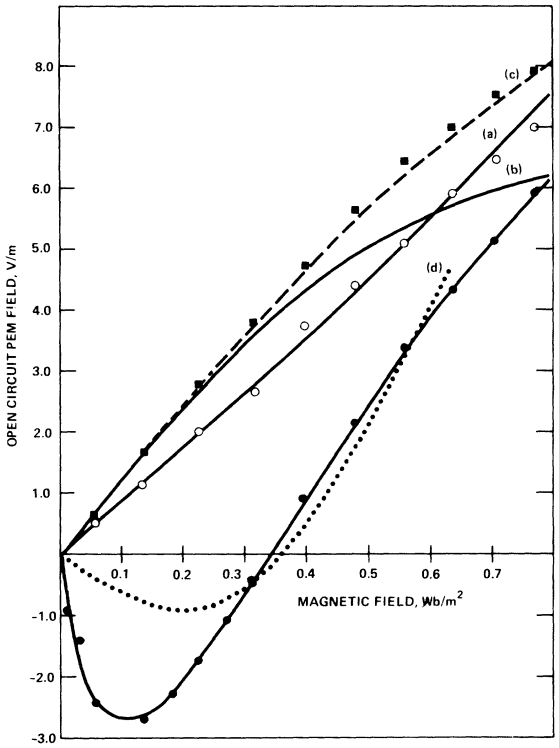

FIG. 9. Magnetic field dependence of the PEM field generated in an anodized sample of InSb. The data have been normalized to an illumination intensity of 1 W/m^2 at a wavelength of 1.65 μm. Room-temperature data ($\times 10^6$) are shown by the open circles and the block points are results at 88 °K ($\times 10^4$). Data ($\times 10^5$) taken at 88 °K following exposure of the anodized surface to room light are shown by the full circles. Positive values correspond to the normal PEM response and negative values to the negative PEM effect. The solid curve (a) is theoretical with $S_1 = 85.0$ m/sec at 300 °K and the solid curve (b) is calculated at 88 °K with $S_1 = 1.35 \times 10^3$ m/sec. The dashed curve (c) is also calculated with these latter values but in this case S_1 was assumed to vary with B as $(1+\mu_h^2 B^2)^{-1/2}$.

response. This value is within one order of magnitude of that previously determined[55] from photovoltage measurements.

Figure 9 shows the magnetic field dependence of the PEM field for the anodized sample at room temperature and at 88 °K both before and after exposure to the high-energy illumination. The lines (a)–(c) are plots of Eq. (17) with appropriate values of S_1. The theoretical curve at room temperature [curve (a)], calculated with $S_1 = 85$ m/sec, can be seen to be in excellent agreement with the experimental data, exhibiting a super linear dependence on B in agreement with the results of Kurnick and Zitter[15] on p-type samples (Both the present n-type material and their p- type is, of course, intrinsic at 300 °K.) The solid curve (b) calculated for $T = 88$ °K and $S_1 = 1.35 \times 10^3$ m/sec (from Fig. 8) does not fit the experimental data at the higher magnetic fields. If, however, a magnetic field dependence of recombination velocity as proposed by Kurnick and Zitter[15] is adopted, i.e., that $S = S(B=0)/(1+\mu_h^2 B^2)^{1/2}$ then the theory, with $S(B=0) = 1.35 \times 10^3$ m/sec, gives the dashed curve (c). Although this dependence can only at this time be postulated, it is felt that the resulting good fit with experiment is significant.

The behavior of the PEM response after room light exposure can be seen to agree qualitatively with the general discussion given earlier, namely, that a sample exhibiting a negative PEM response at low magnetic fields will revert to a normal response for large B. The point at which E_{OC} is zero uniquely defines the corresponding value of S_1 through Eq. (26). In the present case this gives a value of $S_1 = 3.5 \times 10^5$ m/sec. This value however, does not give a good quantitative fit of the

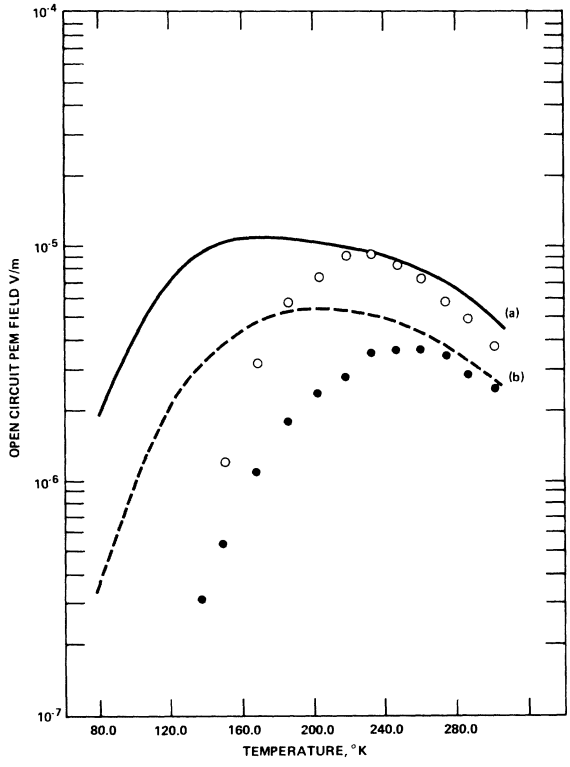

FIG. 10. Open circuit PEM field in a 3.5-μm-thick sample of n-type InSb in a magnetic field of 0.136 Wb/m^2 and an illumination intensity of 1 W/m^2 at 1.65 μm. The open data points are for a bromine in methanol prepared surface and the full circles are for a surface prepared by polishing with No. 2 alumina abrasive. Curve (a) is calculated with values of S_1 as shown by curve (b) in Fig. 6 and curve (b) used the values of S_1 given by curve (c) in the same figure. The full circles and curve (b) correspond to the negative PEM effect.

theory with the data at other values of B. It is felt that this deficiency of the theory is coupled with the inability of the theory to effectively predict the magnitude of the negative PEM response at low temperature as shown in Fig. 7. To demonstrate, however, that although quantitative agreement be lacking that nevertheless qualitative agreement exists the dotted curve (d) in Fig. 9 is a plot of Eq. (17), with $S_1 = 4.0 \times 10^5$ m/sec and multiplied by a fitting factor to give best agreement at large B.

As a final demonstration of the marked contribution that surface recombination may make to the PEM effect a thin film sample of n-type InSb was prepared first with a surface polished in bromine in methanol and then with a surface polished with the No. 2 alumina abrasive. The film, which was prepared by the technique of zone crystallization,[58] had a thickness of ~ 3.5 μm. From Fig. 2 it is evident that such a thin layer should readily exhibit a negative PEM response at relatively low values of S. The results of this measurement are shown in Fig. 10. It can be seen that the polarity of the two signals (after chemical and mechanical polishing) is indeed opposite and furthermore that the magnitude is almost the same in each case. The curves are theory, once again using Eq. (17) with values of carrier concentration and mobility as determined by Hall measurements. Both these parameters were found to be relatively temperature independent with typical values of $\sim 10^{16}$ cm^{-3} and 7×10^5 cm^2/V sec, respectively. The theoretical curves are based on values for S_1 taken from Fig. 6 [curves (b) and (c)] and on the bulk values for carrier lifetimes. Further, the recombination rate on the rear surface of the film in contact with the glass substrate is assumed to be given by curve (b) in Fig. 6. Finally the hole mobility was assumed to bear the same ratio to the electron mobility as do holes in pure bulk material. Although these assumptions may be questioned, no obvious alternatives would seem to be available.

It is felt that even with these reservations, the agreement between theory and experiment in this extreme case is acceptable, lending support not only to the values of S determined on bulk material and shown in Fig. 6 but also to the general validity of the theory presented earlier.

[1] I. K. Kikoin and M. M. Noskov, Phys. Z. Sowjetunion **5,** 586 (1934).
[2] J. Frenkel, Phys. Z. Sowjetunion **5,** 597 (1934); Phys. Z. Sowjetunion **8,** 185 (1935).
[3] P. Aigrain and H. Bulliard, C.R. Acad. Sci. (Paris) **236,** 595 (1953); C.R. Acad. Sci. (Paris) **236,** 672 (1953).
[4] T. S. Moss, L. Pincherle, and A. M. Woodward, Proc. Phys. Soc. Lond. B **66,** 743 (1953).
[5] T. S. Moss, Proc. Phys. Soc. Lond. B **66,** 993 (1953).
[6] W. W. Scanlon, Phys. Rev. **106,** 718 (1957).
[7] H. Bulliard, Phys. Rev. **94,** 1564 (1954).
[8] S. W. Kurnick, A. J. Strauss, and R. N. Zitter, Phys. Rev. **94,** 1791 (1954).
[9] J. R. Dixon, Phys. Rev. **107,** 374 (1957).
[10] J. Auth, J. Phys. Chem. Solids **18,** 261 (1961).
[11] A. Amith, Bull. Am. Phys. Soc. **4,** 28 (1959); Phys. Rev. **116,** 793 (1959).
[12] C. Hilsum and B. R. Holeman, in *Proceedings of the International Conference on Semiconductor Physics* (Czechoslovakian Academy of Science, Prague, 1960), p. 962; B. R. Holeman and C. Hilsum, J. Phys. Chem. Solids **22,** 19 (1961).
[13] C. M. Hurd, Proc. Phys. Soc. Lond. 79, 42 (1962).
[14] O. Garreta and J. Grosvalet, Prog. Semicond. **1,** 165 (1956).
[15] S. W. Kurnick and R. N. Zitter, J. Appl. Phys. **27,** 278 (1956).
[16] W. van Roosbroeck, Phys. Rev. **101,** 1713 (1956).
[17] R. N. Zitter, Phys. Rev. **112,** 852 (1958).
[18] A. R. Beattie and R. W. Cunningham, Phys. Rev. **125,** 533 (1962).
[19] J. Agraz-G and S. S. Li, Phys. Rev. B **2,** 1847 (1970).
[20] S. S. Li and C. I. Huang, J. Appl. Phys. **43,** 1757 (1972).
[21] W. Gärtner, Phys. Rev. **105,** 823 (1957).
[22] J. Hlávka, Phys. Rev. B **6,** 2325 (1972).
[23] C. Hilsum and A. C. Rose-Innes, *Semiconducting III-V Compounds* (Pergamon, New York, 1961).
[24] O. Madelung, *Physics of III-V Compounds* (Wiley, New York, 1964).
[25] H. J. Hrostowski, F. J. Morin, T. H. Geballe, and G. H. Wheatley, Phys. Rev. **100,** 1672 (1956).
[26] E. H. Putley, *The Hall Effect and Related Phenomena* (Butterworth, London, 1960).
[27] C. Hilsum and R. Barrie, Proc. Phys. Soc. Lond. **71,** 676 (1958).
[28] A. C. Beer, J. Appl. Phys. **32,** 2107 (1961).
[29] R. T. Bate, R. K. Willardson, and A. C. Beer, J. Phys. Chem. Solids **9,** 119 (1959).
[30] H. Ehrenreich, J. Phys. Chem. Solids **9,** 129 (1959).
[31] R. A. Stradling and R. A. Wood, J. Phys. C 3, L94 (1970).
[32] V. Roberts and J. E. Quarrington, J. Electron. **1,** 152 (1955).
[33] D. J. Howarth, R. H. Jones, and E. H. Putley, Proc. Phys. Soc. Lond. B **70,** 124 (1957).
[34] R. A. Laff and H. Y. Fan, Phys. Rev. **121,** 53 (1961).
[35] G. K. Wertheim, Phys. Rev. **104,** 662 (1956).
[36] R. N. Zitter, A. J. Strauss, and A. E. Attard, Phys. Rev. **115,** 266 (1959).
[37] D. N. Nasledov and Yu S. Smetannikova, Fiz. Tverd. Tela **4,** 110 (1962) [Sov. Phys.-Solid State **4,** 78 (1962)].
[38] J. E. L. Hollis, S. C. Choo, and E. L. Heasell, J. Appl. Phys. **38,** 1626 (1967).
[39] The number of papers on lifetime in InSb are too numerous to list each individually here. The interested reader is referred to Refs. 34-38 where most of the previous work is considered and to the review article by P. W. Kruse, in *Semiconductors and Semimetals* (Academic, New York, 1970), Vol. 5, p. 15.
[40] A. R. Beattie and P. T. Landsberg, Proc. R. Soc. A **258,** 486 (1960).
[41] B. O. Seraphin and H. E. Bennett, in *Semiconductors and Semimetals* (Academic, New York, 1967), Vol. 3, p. 499.
[42] H. R. Philipp and H. Ehrenreich, Phys. Rev. **129,** 1550 (1963).
[43] T. S. Moss, S. D. Smith, and T. D. F. Hawkins, Proc. Phys. Soc. Lond. B **70,** 776 (1957).
[44] G. W. Gobeli and H. Y. Fan, Phys. Rev. **119,** 613 (1960).
[45] F. P. Kesamanly, Yu. V. Mal'tsev, D. N. Nasledov, Yu. I. Ukhanov, and A. S. Filipchenko, Fiz. Tverd. Tela **8,** 1176 (1966) [Sov. Phys.-Solid State **8,** 938 (1966)].
[46] W. G. Spitzer and H. Y. Fan, Phys. Rev. **106,** 882 (1957).
[47] J. Tauc, J. Phys. Chem. Solids **8,** 219 (1959); J. Tauc and A. Abraham Czech. J. Phys. **9,** 95 (1959).
[48] T. S. Moss, J. Electron. **1,** 126 (1955).
[49] C. Hilsum, D. J. Oliver, and G. Rickayzen, J. Electron. **1,** 134

(1955).
[50]C. Hilsum, Proc. Phys. Soc. Lond. **74,** 81 (1959).
[51]J. L. Davis, Bull. Am. Phys. Soc. **6,** 18 (1961).
[52]J. L. Davis, Surf. Sci. **2,** 33 (1964).
[53]D. L. Lile, Solid-State Electron. **14,** 855 (1971).
[54]W. H. Brattain and J. Bardeen, Bell Syst. Tech. J. **32,** 1 (1953).
[55]D. L. Lile, Surf. Sci. **34,** 337 (1973).
[56]L. G. Bir, Fiz. Tverd. Tela **1,** 67 (1959) [Sov. Phys.-Solid State **1,** 62 (1960)].
[57]V. A. Petrusevich, O. V. Sorokin, and V. I. Kruglov, Fiz. Tverd. Tela 3, 2023 (1961) [Sov. Phys.-Solid State 3, 1470 (1962)].
[58]For a review of this method of film preparation see A. R. Billings, J. Vac. Sci. Tech. **6,** 757 (1969); H. H. Wieder, *Intermetallic Semiconducting Films* (Pergamon, New York, 1970).